

Thickness Dependent Dielectric Strength of a Low-permittivity Dielectric Film

H. K. Kim and F. G. Shi

The Henry Samueli School of Engineering
University of California, Irvine, CA

ABSTRACT

The dielectric strength of a promising interlevel low relative permittivity dielectric is investigated for various film thicknesses and temperatures by using I - V measurements with metal-insulator-semiconductor (MIS) structures. It is found that the dielectric breakdown mechanism also depends on thickness. For relatively thick films (thickness >500 nm), the dielectric breakdown is electromechanical in origin, *i.e.* the dielectric strength is proportional to the square root of Young's modulus of the films. By scanning electron microscopy (SEM) observation, a microcrack in thicker films may contribute to a lower value of Young's modulus, which may confirm that the electromechanical breakdown is the dominant mechanism for dielectric breakdown of thicker films. In addition, the thickness dependent dielectric strength can be described by the well-known inverse power-law relation by using different exponents to describe different thickness ranges. However for thinner films, *i.e.* <500 nm, the experimentally observed relationships among the dielectric strength, Young's modulus, and film thickness cannot be explained by the existing models.

1 INTRODUCTION

THE need for new low relative permittivity materials that can replace silicon dioxide as insulator in a future integrated circuit (IC) device already has started many efforts. As IC device sizes decrease, thinner and thinner dielectric films will be employed for insulation. As expected, the constraints imposed by thin polymer film geometry will lead to the deviation of film properties from that of their bulk counterparts. Recent studies on various low relative permittivity materials have demonstrated that most of structural, optical, mechanical, electrical, dielectric, and thermal properties of polymer films are expected to be film thickness dependent [1-7]. Hence, the film thickness dependence of the key properties of dielectric films becomes an important IC issue [8, 9].

Dielectric strength is always a vital factor in insulation. However, no investigation has been reported on the thickness dependent dielectric strength of low relative permittivity materials for submicrometer interlevel dielectric applications. In this paper, we present our results on thickness and temperature dependent dielectric strength of on-wafer polytetrafluoroethylene (PTFE) thin films, which has the lowest value among the nonporous low relative permittivity materials [8-15]. PTFE thin films ranging in thickness from 90 to 1200 nm were investigated by using the current ramping voltage technique with MIS structures. The observed dielectric strength will be analyzed with respect to fit various models in different thickness ranges. It is also discussed in relation to the microstructure and morphology of the films, as characterized by

X-ray diffraction (XRD), Fourier transform infrared (FTIR) and scanning electron microscopy (SEM).

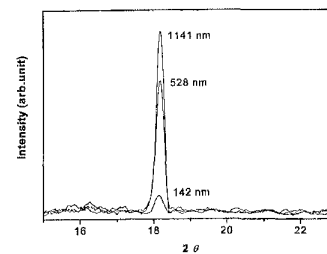


Figure 1. XRD pattern of crystalline PTFE thin film.

2 EXPERIMENTAL

All PTFE dielectric films were spin-coated on the silicon wafers and then baked and sintered on a computer controlled hot plate for 3 min with a curing temperature of 390°C. Samples of different thicknesses (94, 142, 200, 528, 800, and 1141 nm) have been prepared to investigate the dielectric strength dependence. An ellipsometer has been used to measure the thickness of films.

The dc breakdown voltage was measured using MIS structures in air. The dc voltage was applied to the sample, increasing at a linear rate and the dielectric breakdown voltage was measured. For the temperature dependent dielectric strength, all electric stressing was performed

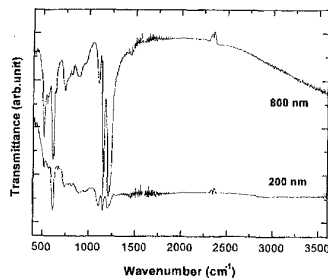


Figure 2. FTIR spectra of crystalline PTFE thin film.

at three temperatures: 25°C, 75°C, and 150°C. The temperature was controlled with an Athena XT16 temperature controller with a type K thermocouple thermometer.

Microstructure and morphology were investigated to elucidate its relation to the dielectric strength of the film. X-ray diffraction (XRD) was performed by using a Siemens D5000 diffractometer with $\text{CuK}\alpha$ irradiation. FTIR spectra were measured by Midac (PRS 102) over the range of 4000 cm^{-1} to 400 cm^{-1} . The measurement is carried out with a resolution of 4 cm^{-1} and the scan is done as many as 32 times. All spectra were collected at room temperature, in an air-tight sample holder. A scanning electron microscope (Philips XL 30 FEG) was used to obtain photomicrographs from gold-coated sample surfaces.

3 RESULTS AND DISCUSSIONS

3.1 MICROSTRUCTURE, MORPHOLOGY OF PTFE FILMS

The key property of a polymer thin film for electrical insulation is its dielectric strength. It is affected by various factors, including the polymer structure and the sample geometry. The phase information of the film was studied by XRD. Figure 1 shows typical 2θ XRD patterns of PTFE thin films of three selected thicknesses [13, 16]. For all three (142, 528, and 1141 nm) samples, the typical (100) peak at 18° is observed which indicates that the film is crystallized, and the basic crystal structure is the same with all samples. However, it was found that intensity of the (100) peak increases with increasing film thickness, which is evidence of both a lower crystalline order than expected in the 142 nm specimen (possibly due to substrate interaction), and an increase in apparent crystallinity at 1141 nm specimen due to thickness. Further, the full-width half maximum (FWHM) of the (100) peak tends to narrow with increasing film thickness, which suggests an increase in the average crystallite size. The crystallite size was calculated from Scherrer's formula, $D=0.9\lambda/B \cos \theta$, with D the crystallite size, λ the wavelength of the incident X-rays, B is the FWHM, and θ the angle of the peak, by using a Lorentz shape fit. It gives a crystallite size of 36, 38, and 39 nm for 142, 528, and 1411 nm specimens, respectively. The presence of the intense (100) peak in the XRD pattern overall 2θ ranges also indicates that the molecular chains are parallel to their substrate surface.

Figure 2 shows the FTIR spectra of the PTFE film with two different film thicknesses, 200 and 800 nm. There is a strong band in the region

of 1000 to 1300 cm^{-1} which is assigned to the asymmetrical and symmetrical CF_2 stretching vibrations. The CF_2 wagging mode is observed at 635 cm^{-1} and the CF_2 bending and rocking modes appear at 500 to 600 cm^{-1} , which are considerably weaker. The bands in the region of 1400 to 1900 cm^{-1} and around 2360 cm^{-1} on the spectra of the film are due to H_2O and CO_2 in air, respectively. The peaks at 3000 cm^{-1} can be assigned to the CH , CH_2 , and CH_3 stretching vibration. Additionally, peaks of the symmetrical and asymmetrical CF_2 stretching vibration mode and the CF_2 wagging mode are relatively strong which is a typical characteristic of crystalline structure of PTFE thin films. As shown, the spectrum over the whole range becomes more pronounced as the thickness of film increases, indicating an increase in the structural order and a higher conformation of the polymer layer in the preferred orientation along the substrate surface.

Figure 3 shows a typical SEM micrograph of the PTFE film. The film is formed by tightly packed parallel helices of long PTFE molecules which conform to the surface structure, and a mature lamellar structure can be observed in thicker films (528 and 800 nm). The shape of the lamella is not like the shapes reported [13, 17, 18], but instead has a worm-like shape. These worm-like shapes are connected together and may not be the same as in the bulk. For thicker films (528 and 800 nm), the film displays the 'fold-over' of the crystalline lamella, which would be considered to reflect the degree of the order with a repeat period. However, for thinner films (94 and 142 nm), a lamella conforms on the top of the thin layer, and some of the helices of PTFE molecules are reentrant, which probably indicate the degree of disorder. Therefore, the lamella is nucleated on the surface of the top ultrathin layer of PTFE crystal, and grows three-dimensionally. Hence, this thickness dependent morphology may lead to the thickness dependence of other properties.

3.2 DIELECTRIC STRENGTH OF PTFE THIN FILMS

3.2.1 THICKNESS DEPENDENCE

I - V measurements were performed for samples with area $1\times 1\text{ cm}^2$. Figure 4 shows the variation of the dielectric strength of PTFE films as a function of the film thickness, which can be fitted well by the following well-known relationship [6, 19-21],

$$E_B \propto h^{-n} \quad (1)$$

where E_B is the dielectric strength, h the film thickness, and n is the fitting parameter. The n factor can be varied with experimental configuration, and may be related to microscopic structure and charge transfer. It also has been discussed in terms of the electron affinity [6, 19, 21, 22].

Equation (1) is known to correlate with the breakdown strength and film thickness for thick polymer films [6, 19], but it is the first time to demonstrate that Equation (1) is also valid for sub-micron thickness low- ϵ polymer films. As indicated, the dielectric strength decreases with increasing thickness. For an ultrathin film thickness ($h < 100\text{ nm}$), the film has the a strength $> 10\text{ MV/cm}$ at room temperature. In thinner regions with more grain boundary volume (small grain size), the lower the local field across the boundary, the higher the dielectric breakdown strength. In thicker films, the higher crystalline order (Figure 1 by XRD observation) can cause a weak dielectric strength spot [23].

All data can be well described by Equation (1), but not with a single value of n . In the present case, for a thickness between 90 and 500 nm,

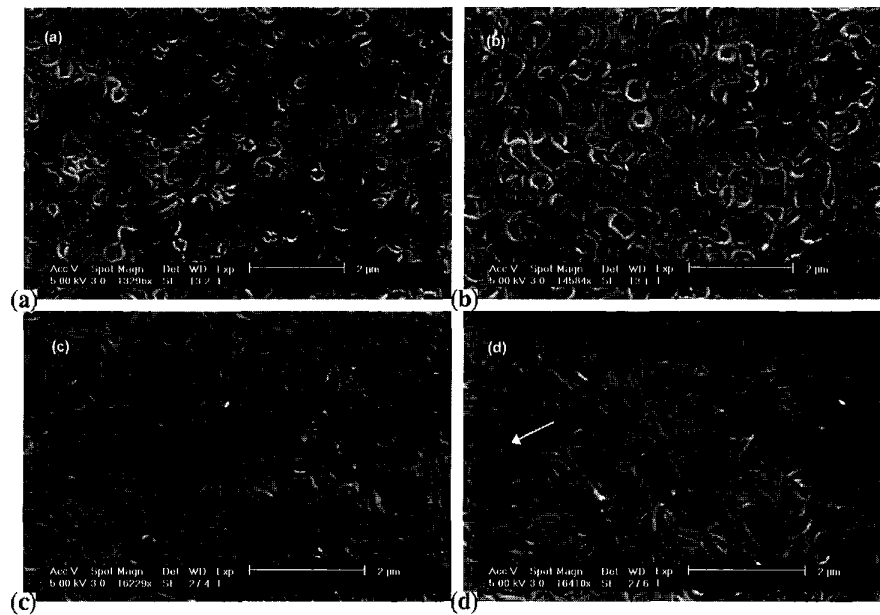


Figure 3. SEM images of crystalline PTFE thin film with thicknesses of (a) 94, (b) 142, (c) 528, and (d) 800 nm.

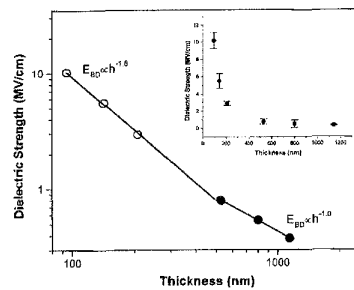


Figure 4. Thickness dependent dielectric strength of PTFE thin films.

$n=1.5$ and $n=1.0$ for the thickness between 500 and 1200 nm. The value for the thinner thickness range is relatively larger than the reported values, ~ 0.5 to 1.0 , at room temperature [19–21], but the value for thicker specimens is in the range of the reported values.

The morphological difference for relatively thicker and thinner films also correlated with the observed difference in the dielectric strength of different thicknesses. From SEM observation, as presented by Figure 3, it is evident that the morphology for relatively thinner films is totally different from that of thicker films. The well-attached structure of the top layer was observed for thinner films (Figures 3(a) and (b)), and a homogeneous surface with mature lamella was observed for thicker films (Figures 3(c) and (d)). This difference may relate to two breakdown regions; a relatively high n value for $h < 500$ nm, and a relatively low n value for $h > 500$ nm. Furthermore, thinner films with the well-conformed structure show a higher dielectric strength.

The film thickness effect has been related to charge trapping and de-trapping [24, 25], material structure, morphology, and for polymers, the value of n depends on the electron affinity [19]. For relatively thinner

films, trapped charges can flow easily because trapped charges do not accumulate within the insulator due to its small size. Hence, a higher electric field is needed to induce electron avalanches.

3.2.2 ELECTROMECHANICAL BREAKDOWN MECHANISM

There is much similarity between mechanical property and dielectric strength. In general, when the insulation is under electric stress, a mechanical stress also is produced. If the strain energy released at electric stress is higher than that required for the deformation of materials, mechanical crack propagation is introduced. Since the mechanical stress also can alter the dielectric strength of materials, the factor that can affect the mechanical property, also can affect the dielectric strength [26, 27]. Figure 5 presents Young's modulus as a function of the film thickness at room temperature. Mechanical properties were measured by using the dynamic contact module (DCM) option of the Nano Indentor XP [3]. As a result, Young's modulus decreases with increasing film thickness, like the dielectric strength decreases with increasing film thickness (Figure 4). Additionally, Young's modulus has two regions that show a similar behavior with the dielectric strength.

For thinner films, their confinement to a surface structure can be attributed to a higher Young's modulus. Additionally, for thicker films, by SEM observation, a microcrack (Figure 3(d) at the arrow) can induce a localized bond breaking [28]. Therefore, the energy required to cause dielectric breakdown will be decreased, and Young's modulus would be less than that of thinner films. Lower values of Young's modulus may suggest that the electromechanical breakdown is the dominant mechanism for the dielectric breakdown of thicker films.

The relation between the dielectric strength and Young's modulus is shown in Figure 6. For thicker films, the relationship between the dielectric strength and Young's modulus according to the electrome-

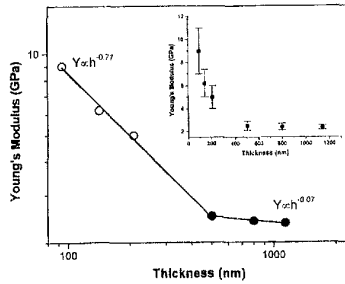


Figure 5. Young's modulus as a function of the film thickness.

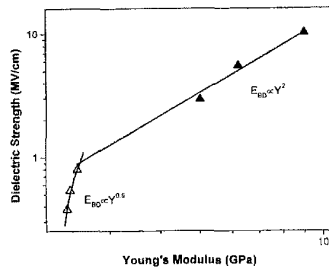


Figure 6. Dielectric strength as a function of Young's modulus.

chanical breakdown theory [26, 29–31] is

$$E_B \propto Y^{1/2} \quad (2)$$

where Y is Young's modulus.

This result presented in Figure 6 thus supports the electromechanical breakdown mechanism for the relatively thicker films. However, the relationship between E_B and Y for thinner films cannot be fitted with Equation (2). Thus there is a fundamentally different breakdown mechanism for the relatively thinner films. The exact mechanism remains to be investigated.

3.2.3 TEMPERATURE DEPENDENCE

The thermal energy is another external stress, added to that of the charge distribution. Due to the structural change with increasing temperatures, the liberated free electrons in the polymer accelerate, and lower its dielectric strength. At very low temperature, all charged particles are trapped. When the temperature is increased, the trapped electrons will be detrapped more easily, and less electric field is needed.

Further, when the temperature increases, the overall volume of samples will expand, and the dielectric strength decreases with the decrease of the film density. Thus, it is expected that E_B decreases with increasing temperature, exactly as observed in the present case of PTFE thin films, shown in Figure 7. The dielectric strength decreases with increasing temperature at all sample thickness ranges. From the inserted graph in Figure 7, the activation energy of dielectric strength increases with increasing film thickness for thinner film thickness range, *i.e.* 0.004 eV for 90 nm, 0.017 eV for 142 nm, and 0.030 eV for 200 nm. However, the activation energy is almost constant for thicker films, *i.e.* 0.035 eV to 0.039 eV for 500 nm to 1200 nm. This is consistent with the suggestion that the dielectric strength is less sensitive to temperature for thicker

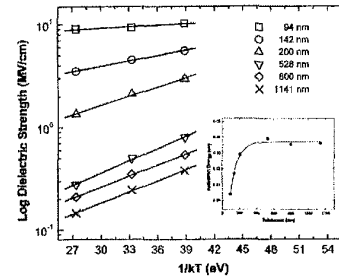


Figure 7. Temperature dependent dielectric strength of PTFE thin films.

films since the electromechanical breakdown is the dominant mechanism for the dielectric breakdown.

This different behavior at high and low temperatures also can be explained by the morphology of the samples. For thinner films, the strong attachment due to their confinement by a surface structure gives high resistance for thermal stress. Hence, the thinnest film (94 nm) shows a relatively lower activation energy compared to thicker films (141 and 200 nm).

4 CONCLUSIONS

THE thickness and temperature dependent dielectric strength of low relative permittivity PTFE polycrystalline thin films on Si substrates in the thickness range of 90 to 1200 nm have been investigated by means of I - V measurements. The dielectric strength decreases with increasing film thickness, which is found to vary as h^{-n} (h being the film thickness). In particular, two regions have been observed with two different n values; a relatively high one, *i.e.* 1.5 for $h < 500$ nm, and a relatively low n value, *i.e.* 1.0 for $h > 500$ nm. The dielectric breakdown for the relatively thicker film range, *i.e.* $500 < h < 1200$ nm, is controlled by the electromechanical breakdown mechanism, as demonstrated by $E_B \propto Y^{1/2}$. However, the relationship among the dielectric strength, Young's modulus, and the film thickness for thinner films, *i.e.* < 500 nm, cannot be explained by the existing models. The exact cause for the observed behavior remains to be investigated. Additionally, the observed two dielectric strength regions can be explained by microstructural and morphological studies. The dielectric strength also has been found to decrease with increasing temperatures for all sample thicknesses. The activation energy of dielectric strength increases with increasing film thickness for the thinner film thickness range. However, the activation energy is almost constant for the thicker films. This is consistent with the suggestion that the dielectric strength is less sensitive to temperature for thicker films, since the electromechanical breakdown is the dominant mechanism.

ACKNOWLEDGMENT

This work is supported by the State of California Microelectronics Innovation and Computer Research Opportunities (MICRO) program.

REFERENCES

- [1] D. T. Hsu, H. K. Kim, F. G. Shi, B. Zhao, M. Brongo, P. Schilling and S. -Q. Wang, "ILD thermal stability in deep-submicron technologies: from thin to ultrathin di-

- electric films", Proc. of the SPIE Conf. on Multilevel Interconnect Technology III, Vol. 3883, pp. 60-67, 1999.
- [2] D. T. Hsu, F. G. Shi, B. Zhao and M. Brongo, "Theory for the thickness dependent glass transition temperature of amorphous polymer thin films", Proc. of the Fourth Intl. Symp. of Low and High Dielectric Constant Materials: Materials Science, Processing, and Reliability Issues, Vol. 99-7, pp. 53-61, 2000.
- [3] J. Wang, F. G. Shi, T. G. Nieh, B. Zhao, M. Brongo, S. Qu and T. Rosenmayer, "Thickness dependence of elastic modulus and hardness of on-wafer low-k ultrathin polytetrafluoroethylene films", Scripta Mater., Vol. 42, pp. 687-694, 2000.
- [4] J. Wang, H. K. Kim, F. G. Shi, B. Zhao and T. G. Nieh, "Thickness dependence of morphology and mechanical properties of on-wafer low-k PTFE dielectric films", Thin Solid Films, Vol. 377, 378, pp. 413-417, 2000.
- [5] D. T. Hsu, H. K. Kim, F. G. Shi, B. Zhao and M. Brongo, "Thickness-dependent dielectric properties of low-k materials", Proc. of the Fourth Intl. Symp. of Low and High permittivity Materials: Materials Science, Processing, and Reliability Issues, Vol. 99-7, pp. 62-68, 2000.
- [6] H. K. Kim, F. G. Shi, B. Zhao, and M. Brongo, "Low-k Dielectrics for ULSI Multilevel Interconnections: Thickness-Dependent Electrical and Dielectric Properties", Conf. Record of the 2000 IEEE Intl. Symp. on Electrical Insulation, pp. 62-65, 2000, Piscataway, NJ, USA.
- [7] G. Yilmaz and O. Kalenderli, "Dielectric behavior and electric strength of polymer films in varying thermal conditions for 5 Hz to 1 MHz frequency range", Proc. of Electrical Insulation Conf. and Electrical Manufacturing and Coil Winding Conf., pp. 269-271, 1997.
- [8] R. D. Miller, "Device physics - In search of low-k dielectrics", Science, Vol. 286, pp. 421-423, 1999.
- [9] E. T. Ryan, A. J. McKerrow, J. P. Leu and P. S. Ho, "Materials issues and characterization of low-k dielectric materials", MRS Bulletin, Vol. 22, pp. 49-54, 1997.
- [10] T. Rosenmayer and H. Kosugi, "Thermal desorption spectroscopy of PTFE dielectric films deposited on silicon wafers", Dielectric Material Integration for Microelectronics, Vol. 98-3, pp. 88-94, 1998.
- [11] L. Peters, "Pursuing the perfect low-k dielectric", Semiconductor Int I., Vol. 21, pp. 64-74, 1998.
- [12] H. Usui, H. Koshikawa and K. Tanaka, "Characteristics of polytetrafluoroethylene thin films prepared by ionization-assisted deposition", IEICE Transactions on Electronics, Vol. E81-C, pp. 1083-1089, 1998.
- [13] S. T. Li, E. Arenholz, J. Heitz and D. Bauerle, "Pulsed-laser deposition of crystalline Teflon (PTFE) films", Applied Surface Science, Vol. 125, pp. 17-22, 1998.
- [14] S. C. Sun, Y. C. Chiang, C. T. Rosenmayer, J. Teguh and H. Wu, "Evaluation of PTFE nanoemulsion as a low permittivity material ILD", Proc. of Symp. of Low-permittivity Materials, pp. 85-90, 1997.
- [15] C. T. Rosenmayer, J. W. Bartz and J. Hammes, "Adhesion and dielectric strength of ultralow-dielectric-constant PTFE thin films", Proc. of Symp. of Low-permittivity, pp. 231-236, 1997.
- [16] Y. Ueno, T. Fujii and F. Kannari, "Deposition of fluoropolymer thin films by vacuum-ultraviolet laser ablation", Appl. Phys. Lett., Vol. 65, pp. 1370-1372, 1994.
- [17] R. Schwodiauer, S. Bauer-Gogonea, S. Bauer, J. Heitz, E. Arenholz and D. Bauerle, "Charge stability of pulsed-laser deposited polytetrafluoroethylene film electrets", Appl. Phys. Lett., Vol. 73, pp. 2941-2943, 1998.
- [18] T. Katoh and Y. Zhang, "Synchrotron radiation ablative photodecomposition and production of crystalline fluoropolymer thin films", Appl. Phys. Lett., Vol. 68, pp. 865-867, 1996.
- [19] B. Helgee and P. Bjellheim, "Electric breakdown strength of aromatic polymers: dependence on film thickness and chemical structure", IEEE Transactions on Electrical Insulation, Vol. 26, pp. 1147-1152, 1991.
- [20] V. K. Agarwal and V. K. Srivastava, "Thickness dependent studies of dielectric breakdown in Langmuir thin molecular films", Solid State Communications, Vol. 12, pp. 829-834, 1973.
- [21] G. Damamme and C. Le Gressus, "Effect of the insulator size on the breakdown strength", IEEE 1997 Annual Report Conf. on Electrical Insulation and Dielectric Phenomena, Vol. 1, pp. 92-95, 1997.
- [22] V. K. Agarwal and V. K. Srivastava, "Thickness dependence of breakdown field in thin films", Thin Solid Films, Vol. 8, pp. 377-381, 1971.
- [23] M. Araoka, H. Yoneda and Y. Ohki, "Dielectric breakdown of new type polymerized polyethylene using a single-site catalyst", IEEE Transactions on Dielectrics and Electrical Insulation, Vol. 6, pp. 326-330, 1999.
- [24] K. H. Oh, C. K. Ong, B. T. G. Tan, C. Le Gressus and G. Blaise, "Variation of trapping/detrapping properties as a function of the insulator size", J. Appl. Phys., Vol. 74, pp. 1960-1967, 1993.
- [25] G. Blaise, "Charge trapping/detrapping induced lattice polarization/relaxation processes", Proc. of 1995 Conf. on Electrical Insulation and Dielectric Phenomena, pp. 37-39, 1995.
- [26] S. Jeffery, C. J. Sofield and J. B. Pethica, "The influence of mechanical stress on the dielectric breakdown field strength of thin SiO₂ films", Appl. Phys. Lett., Vol. 73, pp. 172-174, 1998.
- [27] G. R. Greenway, A. S. Vaughan and S. M. Moody, "Morphology and the electro-mechanical breakdown model in polyethylene", Conf. on Electrical Insulation and Dielectric Phenomena, Vol. 2, pp. 666-669, 1999.
- [28] T. J. Lewis, "New electro-mechanical concepts of the primary mechanisms of electrical breakdown in liquids", ICDL'96 12th Intl. Conf. on Conduction and Breakdown in Dielectric Liquids, pp. 273-278, 1996.
- [29] M. Hikita, S. Tajima, I. Kanno, I. Ishino, G. Sawa and M. Ieda, "High-field conduction and electrical breakdown of polyethylene at high temperatures", Japan J. Appl. Phys., Vol. 24, pp. 988-996, 1985.
- [30] K. H. Stark and C. G. Garton, "Electric strength of irradiated polyethylene", Nature, Vol. 176, pp. 1225-1226, 1955.
- [31] J. C. Fothergill, "Filamentary electromechanical breakdown", IEEE Transactions on Electrical Insulation, Vol. 26, pp. 1124-1129, 1991.

Manuscript was received on 3 June 2000, in final form 12 December 2000.